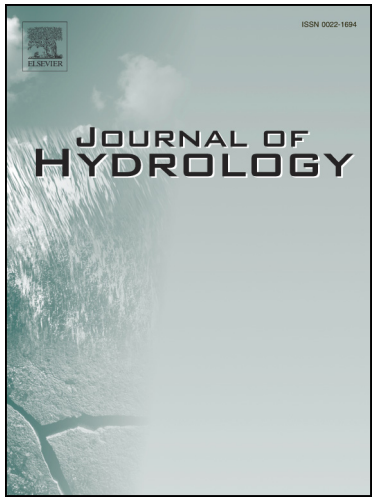

Research papers

Estimating hydrological parameters based on rainfall patterns in river basins with no long-term historical observations

Haiyun Shi, Tiejian Li

PII: S0022-1694(17)30563-2
DOI: http://dx.doi.org/10.1016/j.jhydrol.2017.08.030
Reference: HYDROL 22193

To appear in: *Journal of Hydrology*

Received Date: 27 May 2017
Revised Date: 19 July 2017
Accepted Date: 19 August 2017

Please cite this article as: Shi, H., Li, T., Estimating hydrological parameters based on rainfall patterns in river basins with no long-term historical observations, *Journal of Hydrology* (2017), doi: http://dx.doi.org/10.1016/j.jhydrol.2017.08.030

Estimating hydrological parameters based on rainfall patterns in river basins with no long-term historical observations

Haiyun SHI [a,b,c], Tiejian LI [b,c]

[a]*Department of Civil Engineering, The University of Hong Kong, Hong Kong, China*

[b]*State Key Laboratory of Hydroscience and Engineering, Tsinghua University, Beijing, China*

[c]*State Key Laboratory of Plateau Ecology and Agriculture, Qinghai University, Xining, Qinghai, China*

E-mail address: shihaiyun_2013@tsinghua.org.cn

Telephone: (00852)-2859-1970

Fax: (00852)-2559-5337

Revised manuscript for the *Journal of Hydrology*

July 2017

Abstract

Small and medium river basins may frequently suffer from the destructive hydrological extremes (e.g., floods). However, the common problem in such regions is a lack of long-term historical observations. Meteorological and hydrological station networks in some river basins in China were newly-built only a few years ago, and it is infeasible to estimate hydrological parameters from calibration and validation with a long time period directly. This paper aims to develop a method to estimate the feasible hydrological parameters based on rainfall patterns in such regions. Digital Yellow River Integrated Model (DYRIM) is adopted as the hydrological model, and the feasible hydrological parameters can be estimated based on limited rainfall-runoff events. First, for each rainfall-runoff event, the parameters are independently calibrated with the observed rainfall and hydrological data using a double-layer parallel system. Then, the performances of the simulation results are comprehensively evaluated, and the value ranges of the parameters can be obtained. Finally, the statistical relationships between hydrological parameters and rainfall patterns (i.e., amount and intensity) are established, which are expressed by the statistical equations and the distribution of hydrological parameters with the rainfall patterns. From a sample demonstration, it is concluded that this parameter estimation method will be useful to estimate the feasible hydrological parameters for future rainfall-runoff events in river basins with no long-term historical observations.

Keywords: Hydrological parameter estimation; Rainfall patterns; Digital Yellow River Integrated Model (DYRIM); Small and medium river basins.

1. Introduction

Hydrological extremes (e.g., floods) in small and medium river basins are regarded as an important factor that can affect the social and economic development. In such regions, high-intensity rainstorms frequently occur during the rainy season, which may lead to serious flood disasters and cause enormous losses of lives and property (Liu et al., 2010; Ye et al., 2012; Shi et al., 2015). However, the mechanism of the occurrence of rainstorms is quite complicated so that it is difficult to have an in-depth understanding of it. Moreover, another problem in such river basins is a lack of long-term historical observations (e.g., Skaugen et al., 2015; Athira et al., 2016; Garambois et al., 2017; Yoo et al., 2017). For example, the meteorological and hydrological station networks in some small and medium river basins in China are usually poor. No meteorological and hydrological stations can be found in some river basins; even if there are several stations, the series of the observed data are usually not long enough for calibration and validation of hydrological models with a long time period. Consequently, more technical and financial supports should be provided for such river basins; moreover, it is important and necessary to develop an effective method to estimate hydrological parameters in river basins with no long-term historical observations.

In the past few years, many researchers have made efforts to address this problem in ungauged or poorly gauged river basins (e.g., Bardossy, 2007; Hundecha et al., 2008; Bulygina et al., 2012; Woldemeskel et al., 2013; Shi et al., 2015; Yu et al., 2016; Gao et al., 2017; Garambois et al., 2017; Yoo et al., 2017), mainly focusing on the following two types of methods. The first type is the methods based on regional information representing

river basin characteristics (e.g., Bardossy, 2007; Hundecha et al., 2008; Bulygina et al., 2012; Yoo et al., 2017). It is supposed that river basins with similar characteristics may show a similar hydrological behavior and thus can be simulated with similar hydrological parameters. As a result, hydrological parameters in an ungauged or poorly gauged river basin can probably be transferred from a reference river basin which is adjacent or has similar characteristics with this river basin (Bardossy, 2007; Tang et al., 2010). Moreover, for a designated river basin, correlation analysis between hydrological parameters and river basin characteristics can be conducted to improve the model performance (e.g., Merz and Blöschl, 2005; Wagener and Wheater, 2006; Coff et al., 2009; Bulygina et al., 2012). For example, using a formal Bayesian procedure, Bulygina et al. (2012) combined three different sources of knowledge (i.e., physical properties, regionalized signatures of flow and available flow measurements) into a distributed model for a river basin in the UK and found that the physical properties source could contribute most to improving the model performance. Recently, the global-scale satellite-based meteorological datasets have been developed rapidly with the development of science and technology, which are regarded to be an effective supplement for the gauge-station measurements (e.g., Pappenberger et al., 2008; Li et al., 2012; Woldemeskel et al., 2013). Hence, the second type is the methods based on the utilization of the satellite-based meteorological datasets (e.g., Shi et al., 2015; Yu et al., 2016; Gao et al., 2017). For the river basins with poor historical observations, especially for the ungauged river basins, the satellite-based meteorological datasets may provide the necessary input data to overcome the problem of lacking data when estimating the hydrological parameters through calibration and validation of models (e.g., Sun et al., 2012; Maswood and Hossain, 2016; Garambois et al., 2017).

In China, an increasing number of meteorological and hydrological station networks have been built in some small and medium river basins to acquire the necessary data for hydrological simulation; however, due to the lack of long-term historical observations, it is still difficult to estimate the hydrological parameters from calibration and validation of hydrological models with a long time period directly. To this end, this paper aims to propose a feasible hydrological parameter estimation method in such river basins through establishing the relationships between hydrological parameters and rainfall patterns (i.e., amount and intensity). A physically-based hydrological model, the Digital Yellow River Integrated Model (noted as DYRIM hereafter) (Wang et al., 2007, 2015; Li et al., 2009), is adopted in this paper to conduct hydrological simulations, and the Leli River basin, a sub-basin of the Pearl River basin in China, is selected as the study area. From a sample demonstration, it is concluded that the proposed method will be useful to estimate the feasible hydrological parameters for future rainfall-runoff events in such river basins. The remainder of this paper is organized as follows. Section 2 shows the main methodologies. Section 3 gives a brief introduction to the study area and research data. Section 4 shows results and discussion of the case study. The final section displays the conclusions of this paper.

2. Methodology

2.1. The hydrological parameter estimation method

In order to conduct hydrological simulations using distributed hydrological models, the applicable hydrological parameters for the designated river basin should be determined first. Normally, they can be calibrated and validated with long-term historical observations;

however, with respect to small and medium river basins with few available observations, such method will probably be invalid. Therefore, in consideration of the uncertainty of the hydrological parameters, the hydrological parameter estimation method for river basins with no long-term historical observations is proposed based on the rainfall patterns derived from limited rainfall-runoff events (Figure 1). In this paper, the rainfall-runoff events (i.e., the flood events in the subsequent sections) are selected based on the observed streamflow data. For a designated river basin, the observed streamflow data is equal to the base flow of this river basin during the period with no rain. When the rain occurs, there is a significant increase in the observed streamflow data until reaching the peak, and then a decrease in the observed streamflow data until returning to the base flow. Therefore, the day when the observed streamflow data begin to increase can be identified and the day before this day is regarded as the start date of a rainfall-runoff event. Moreover, the day when the observed streamflow data return to the base flow can be identified and the day after this day is regarded as the end date of a rainfall-runoff event. Then, the proposed method involves the following three steps.

Step 1:

For each rainfall-runoff event, the hydrological simulation is conducted using the DYRIM (Wang et al., 2007, 2015), and the hydrological parameters in the DYRIM are independently calibrated with the observed rainfall and hydrological data using a double-layer parallel system for hydrological model calibration (Zhang et al., 2016). In recent years, there have been several studies (e.g., Choi et al., 2015; Reshma et al., 2015; Huang et al., 2016; Fuentes-Andino et al., 2017) on event-based calibration of hydrological models, including some of our previous studies (e.g., Shi, 2013; Zhang et al., 2016).

Step 2:

For each rainfall-runoff event, the performance of the hydrological simulation result is separately evaluated using the selected assessment criteria (see subsection 2.4 for details). Then, all the rainfall-runoff events are regarded as a whole and comprehensive evaluation is conducted to show the overall simulation accuracy. Moreover, the value ranges of the hydrological parameters can be determined from multiple sets of calibrated parameters through identifying the maximum and minimum values.

Step 3:

For each rainfall-runoff event, the rainfall patterns (i.e., amount and intensity) are obtained based on the observed rainfall data. In this paper, the rainfall amounts of all the stations during the period of each rainfall-runoff event are calculated, and then the average rainfall amount over the river basin can be derived using the Thiessen polygon method (Thiessen and Alter, 1911; Brassel and Reif, 1979). In addition, the observed rainfall data recorded at all the stations are converted into the rainfall intensities in millimeters per hour, and then the maximum one can be derived. Correlations between hydrological parameters and rainfall patterns (i.e., amount and intensity) are analyzed, and the variables applicable for establishing the statistical relationships are determined. Using the regression method, the statistical equations including the selected variables can be obtained; moreover, the distributions of hydrological parameters with rainfall patterns can be mapped. Both of them will be valuable for estimating hydrological parameters for future rainfall-runoff events with limited observed data.

2.2. Brief Introduction of the DYRIM

The DYRIM is a physically-based, distributed-parameter, and continuously-simulated model developed by Tsinghua University for hydrological and sediment simulations in river basins based on the high-resolution digital drainage network (Wang et al., 2007, 2015; Li et al., 2009), which is extracted from the 30-m-resolution Advanced Spaceborne Thermal Emission and Reflection Radiometer (ASTER) Global Digital Elevation Model (GDEM) dataset (ASTER GDEM Validation Team, 2011; Bai et al., 2015a, 2015b) and coded by using a modified binary tree method (Li et al., 2010). Regarding the hillslope-channel as the basic hydrological unit, the DYRIM can simulate runoff yield and flow routing on each hillslope-channel unit. Moreover, the dynamic parallelization technology based on sub-basin decomposition has been developed to speed up the simulation (Li et al., 2011; Wang et al., 2011, 2012; Zhang et al., 2016). In our previous studies, the DYRIM has been widely employed to the hydrological and sediment simulations in major river basins of China, such as the Yellow River basin, the Yangtze River basin and the Pearl River basin (Yin, 2009; Shi, 2013; Shi et al., 2011, 2015, 2016; Zhang et al., 2016), which can demonstrate its universal applicability at the time scales ranging from daily to monthly.

The rainfall-runoff model in the DYRIM is established on each hillslope unit, considering two soil layers (i.e., topsoil and subsoil layers) to reflect both the infiltration-excess and storage-excess mechanisms, in fine time steps (e.g., 6 minutes). Infiltration-excess runoff on the hillslope surface, along with related hydrological processes, such as vegetation interception, evapotranspiration, groundwater discharge and water redistribution between the two soil layers, constitute the fundamental hydrological processes simulated

by this model. Moreover, the flow routing is simulated over this drainage network using a diffusive wave method.

The parameters in the ranifall-runoff model can be divided into two types, namely, physical parameters and calibration parameters. Physical parameters, including the field capacity (*CT1*) and the free water content (*CT2*) of the topsoil layer, the field capacity (*CS1*) and the free water content (*CS2*) of the subsoil layer, the depth of topsoil layer (*D*), and the water capacity of unit LAI (*I*), are used to describe the properties of the land use and soil type. These parameters have less influence on the hydrological simulation over a river basin and can be determined from field measurements and handbooks. By contrast, calibration parameters, which are sensitive and adjustable, must be calibrated before model application using the observed data. According to our previous studies (Wang et al., 2015; Shi et al., 2015, 2016), the most important calibration parameters are the vertical saturated conductivity of the topsoil layer (*KVT*), the vertical saturated conductivity between the two soil layers (*KVS*), and the horizontal saturated conductivities of the two soil layers (*KHT* for the topsoil layer and *KHS* for the subsoil layer). Moreover, among the four parameters, the two vertical saturated conductivities (*KVT* and *KVS*) are the key calibration parameters (Wang et al., 2007, 2015; Zhang et al., 2016).

2.3. Calibration of the DYRIM

The model parameters in the DYRIM are automatically calibrated with a double-layer parallel system (Zhang et al., 2016). A dynamic sub-basin decomposition method (Li et al., 2011) was developed to parallelize the hydrological simulation of the DYRIM, which contributes to the lower-layer parallelism. The MPI standard is adopted to realize the

lower-layer parallelism, mainly because it is the dominant technique to develop parallel programs on distributed memory systems. Moreover, the job scheduling functions of an HPC (High Performance Computing) system are used to manipulate simultaneous model executions with different hydrological parameter combinations in the same generation of an optimization algorithm, which contributes to the upper-layer parallelism.

In this paper, the genetic algorithm (GA) (Holland, 1975) is adopted to search the feasible hydrological parameters due to its stability, natural parallelism and problem-independence. Herein the GA implementation treats the parameters to be optimized as real numbers with simulated binary crossover and real-parameter mutation. This technique promises the parameters independent of the GA and easy to be optimized. When the GA needs to evaluate the fitness of various model parameter combinations, the job scheduler of the HPC system is called to put a number of DYRIM jobs with different parameter values into the job list of the HPC and to monitor the job list. When all of the jobs are completed, the model efficiency will be estimated using observed data to propose the fitness evaluation list. Generations of the GA will be run to explore more parameter combinations until the stop criterion is reached (Zhang et al., 2016).

2.4. Assessment Criteria

To evaluate the performances of the hydrological simulation results using the DYRIM, two objective functions are selected as assessment criteria, namely, the *RE* (Relative Error) and the *NSCE* (Nash-Sutcliffe Coefficient of Efficiency) (Nash and Sutcliffe, 1970). The equations for computing these two objective functions are given as follows:

$$RE = (X_{i,\mathrm{sim}} - X_{i,\mathrm{obs}}) / X_{i,\mathrm{obs}} \quad (1)$$

$$NSCE = 1 - \frac{\sum_{i=1}^{N}\left(X_{i,\mathrm{obs}} - X_{i,\mathrm{sim}}\right)^2}{\sum_{i=1}^{N}\left(X_{i,\mathrm{obs}} - \overline{X}_{\mathrm{obs}}\right)^2} \quad (2)$$

where $X_{i,\mathrm{obs}}$ and $X_{i,\mathrm{sim}}$ are the i-th observation and simulation, respectively; $\overline{X}_{\mathrm{obs}}$ is the mean value of the observations; and N is the sample size.

These two objective functions can provide different criteria in evaluating the model performance. The *RE* can indicate the degree of bias between the simulations and observations, and the value of 0 indicates a perfect simulation. The *NSCE* can measure the goodness of fit, and its value approaches 1.0 if the simulations are close to the observations.

In addition, according to the assessment criteria proposed by the Ministry of Water Resources of China (MWR, 2000), the acceptable simulation result for a single rainfall-runoff event should meet the following three criteria at the same time: (1) the *NSCE* value is higher than 0.80, (2) the *RE* of the peak flow (noted as *REPF* hereafter) is within $\pm 10\%$, and (3) the *RE* of the flood volume (noted as *REFV* hereafter) is within $\pm 10\%$. While for a group of rainfall-runoff events, there are three grades of simulation accuracy, i.e., the first grade with the *NSCE* value larger than 0.9, the second grade with the *NSCE* value between 0.70~0.90 and the third grade with the *NSCE* value between 0.50~0.70. The acceptable simulation result should at least meet the requirement of the third grade.

3. Study area and research data

To demonstrate the performance of the proposed hydrological parameter estimation method, the Leli River basin located in Guangxi, China (105°55' - 106°15' E, 24°16' -

24°34' N), is selected as the study area (Figure 2). It is a sub-basin of the Pearl River basin and has a drainage area of 606 km^2. This river basin is a humid region with the multi-year mean precipitation of 1200 mm, and nearly 80% of the annual precipitation occurs during the rainy season from May to October. Moreover, affected by extreme weather events, floods may easily happen in this river basin.

The high-resolution digital drainage network of the Leli River basin extracted from the ASTER GDEM for running the DYRIM is also shown in Figure 2. Within the Leli River basin, there is only one hydrological station (i.e., Tianlin station) built in 2005 (Figure 2), and the observed streamflow data at the hourly time scale are available from 2005 to 2008. In addition, there are four rainfall stations (i.e., Bantao, Geyan, Sanyao and Tianlin stations) built in 2005 within this river basin (Figure 2), and the observed rainfall data at the hourly time scale are available from 2005 to 2008. Based on the observed streamflow data from 2005 to 2008, there are totally 18 floods identified (i.e., 3 floods in 2005, 6 floods in 2006, 5 floods in 2007 and 4 floods in 2008, respectively), regarding the flood occurred during June 20-27, 2005, as the first one, and the flood occurred during July 22-31, 2008, as the last one. In this paper, the 14 floods occurred during 2005-2007 are used to develop the statistical relationships between hydrological parameters and rainfall patterns, while the 4 floods occurred in 2008 are used to validate the proposed relationships.

According to the Soil Map of China (Chinese Academy of Sciences, 1978), the major soil type of the study area is red soil, which has large hydraulic conductivities. Therefore, the soil type of the study area is assumed to be homogeneous in this paper. The vegetation coverage is represented by Global Inventory Modeling and Mapping Studies Normalized Difference Vegetation Index (GIMMS NDVI) data, which are derived from the Advanced

Very High Resolution Radiometer (AVHRR) instrument onboard the National Oceanic and Atmospheric Administration (NOAA) satellite (Tucker et al., 2005).

4. Results and discussion

4.1. Results of hydrological simulations

In this paper, the hydrological simulations of all the 18 floods occurred during 2005-2008 in the Leli River basin are conducted using the DYRIM and the hydrological parameters for each flood event are independently calibrated using the double-layer parallel system. Before the simulations, the physical parameters should be determined, which are primarily derived from the previous study on the Pearl River basin using the DYRIM (Yin, 2009) and further validated based on the observed rainfall and streamflow data in 2005 (see Table 1). Moreover, Yin (2009) has pointed out that the vertical saturated conductivity of the topsoil layer is large and should be higher than 95 mm/hr. Therefore, the *KVT* value is set to be 100 mm/hr to ensure that the runoff yield is under the saturated storage condition, which properly reflects the mechanism of runoff yield in this river basin; while the value ranges of the other three calibration parameters are all set to be 0.01~10 mm/hr, which is wider than those proposed by Yin (2009) to ensure that the reasonable value ranges are included. Moreover, the computational time step and output time step for simulation using the DYRIM are set to be 6 minutes, and the original outputs are averaged in each hour to generate the hourly streamflows, which can be easily compared against the observed streamflow data recorded at the Tianlin hydrological station.

Because each flood event is independently calibrated in order to obtain the optimal hydrological parameters for this event, the performances of calibration are different among

events. Table 2 lists the values of the relevant assessment criteria, i.e., the *NSCE*, *REPF* and *REFV* values, for each flood. It is observed that the simulation accuracy is generally high: (1) the *NSCE* values of 14 floods are higher than 0.5, with the highest value of 0.95 for the flood occurred during June 28 - July 4, 2005; moreover, the overall *NSCE* value of these 14 floods is 0.84; (2) the *REPF* values of 13 floods are within ±20%, with the lowest value of 1% for the flood occurred during August 4-15, 2006 and -1% for the flood occurred during June 26-29, 2007, respectively; (3) the *REFV* values of 14 floods are within ±20%, with the lowest value of -2% for the flood occurred during July 22-31, 2008. However, only the simulation results of two floods, which occurred during July 7-14, 2006 and June 12-14, 2008, can meet the three assessment criteria at the same time: (1) the *NSCE* values are 0.94 and 0.92, higher than 0.80, (2) the *REPF* values are -9% and -2%, within ±10%, and (3) the *REFV* values are 7% and -6%, within ±10%.

Figure 3 shows the comparisons of the simulations against the observations for the 3 floods with the *NSCE* values higher than 0.9. It is observed that both the peak values and the peak times can be well simulated, which indicates the good performance of the model. However, there are also 4 floods with the *NSCE* values lower than 0.5, which indicates that the model performance may not be so good for these floods. In order to investigate the sources of errors, the comparisons of the simulations against the observations for these 4 floods are shown in Figure 4. It is observed that the low *NSCE* values are mainly caused by the discrepancies between the simulated and observed peak flow. The simulated peak values are all much smaller than the observed ones (i.e., -21%, -19%, -44% and -17% for these 4 floods, respectively), and for the 3 floods in Figures 4(a), 4(c) and 4(d), the peak

times are all several hours in advance (i.e., 5, 6 and 4 hours, respectively). By contrast, for the flood in Figure 4(b), there are three observed peak flows, among which, the first one cannot be captured, the second one is captured in the right peak time but much smaller (i.e., -19%), and the third one is captured in the right order of magnitude with a time lag. The major reason for this may be that the spatial and temporal resolutions of the rainfall data used in this paper are not high enough. The mean control area of each rainfall station is approximately 150 km^2, and the time intervals between the adjacent records are mostly 1 hour (or larger). Because rainfall intensity has been proved to have a great impact on hydrological processes (Shi and Wang, 2015), there might be a certain negative impact on the rainfall-runoff simulation since the short-duration and high-intensity rains may be homogenized. Second, the model structure of the DYRIM is regarded as an influencing factor in the simulation accuracy (Shi et al., 2015, 2016).

4.2. Comprehensive evaluation as a group of floods

Normally, a number of floods can be regarded as a group in order to comprehensively evaluate the simulation accuracy. Considering all the 18 floods, the mean *NSCE* value is 0.66, the mean *REPF* value is -9%, and the mean *REFV* value is -5% (see Table 2). In addition, the overall *NSCE* value of all the 18 floods is 0.79, which is approximately equal to 0.80. According to the assessment criteria proposed by the MWR of China (MWR, 2000), such a group of floods can meet the requirement of the third grade for hydrological simulation accuracy even if the mean *NSCE* value (i.e., 0.66, between 0.50~0.70) is used. In consideration of the overall *NSCE* value (i.e., 0.79, between 0.70~0.90), the requirement of the second grade can be met by this group of floods. Moreover, both the mean *REPF*

and *REFV* values are within ±10%, which further indicates the generally high simulation accuracy of this group of floods.

Therefore, the calibration parameters (i.e., *KVS*, *KHT* and *KHS*) after calibrations are regarded as the feasible hydrological parameters for each flood, and Table 3 lists the value ranges of these calibration parameters in this river basin. For the *KVS* value, the value range is 1.2~10.0 mm/hr, with the mean value of 5.5 mm/hr and standard deviation of 2.8 mm/hr. For the horizontal saturated conductivities, the *KHT* value is in the same order of magnitude as the *KVS* value, with the value range of 1.8~9.9 mm/hr, the mean value of 6.2 mm/hr and standard deviation of 2.5 mm/hr. In contrast, the *KHS* value is nearly one order of magnitude smaller than the *KVS* and *KHT* values, with the value range of 0.01~1.0 mm/hr, the mean value of 0.41 mm/hr and standard deviation of 0.3 mm/hr, indicating that the subsoil layer in this river basin is a relatively impermeable layer. Although these three parameters are still changing after calibrations, they are supposed to be distributed with reasonable value ranges (e.g., 1.2~10.0 mm/hr for the *KVS* value, 1.8~9.9 mm/hr for the *KHT* value, and 0.01~1.0 mm/hr for the *KHS* value, respectively).

Furthermore, a significant negative correlation (i.e., the correlation coefficient is -0.60, significance level $p < 0.01$) is found between the *NSCE* value and the *KVS* value, while the correlations of the *NSCE* value with the *KHT* (i.e., the correlation coefficient is -0.04) and *KHS* (i.e., the correlation coefficient is 0.29) values are not statistically significant. This indicates that the *KVS* value is more sensitive than the *KHT* and *KHS* values, which can prove the statement mentioned above that the vertical saturated conductivities are the key calibration parameters (Wang et al., 2007, 2015; Zhang et al., 2016). Figure 5 shows the

relationships of the *NSCE* value with the *KVS*, *KHT* and *KHS* values, as well as the linear regression equations with the R^2 values. The *NSCE* value shows a decreasing trend along with the increase of the *KVS* value, and the R^2 value is 0.36. Moreover, the R^2 values in Figures 5(b) and 5(c) are approximately equal to 0, indicating the rather weak relationships of the *NSCE* value with the *KHT* and *KHS* values.

4.3. Relationships between hydrological parameters and rainfall patterns

The estimation methods of the hydrological parameters under different rainfall patterns have been reported by several previous studies, especially for the extreme rainfall events (e.g., Soulis and Valiantzas, 2012; Chen et al., 2015; Garcia and Koike, 2016). In this paper, the relationships between parameters in hydrological models and rainfall patterns (i.e., amount and intensity) are analyzed using the regression method, and the statistical equations to estimate the feasible hydrological parameters based on the selected rainfall patterns are established.

Based on the observed data recorded at each rainfall station in the Leli River basin, the rainfall patterns (i.e., amount and intensity) during the period of each flood are computed. Table 4 lists the average rainfall amount and the maximum rainfall intensity during the period of each flood in the Leli River basin. The average rainfall amount values are markedly different, and the highest value (i.e., 139.3 mm during June 8-11, 2008) is nearly 3-fold higher than the lowest value (i.e., 45.3 mm during June 13-16, 2006). Moreover, the maximum rainfall intensity values are all lower than 100 mm/hr (i.e., the given *KVT* value in this paper), varying from the lowest value (i.e., 15.7 mm/hr during August 4-15, 2006) to the highest value (i.e., 57.1 mm/hr during June 8-11, 2008). This indicates that setting

the *KVT* value to be 100 mm/hr is high enough to ensure the runoff yield under the saturated storage condition.

The correlations of the average rainfall amount with the *KVS*, *KHT* and *KHS* values are firstly investigated but none of them is significant even at the significance level of $p = 0.1$, which indicates that these parameters cannot be estimated based on the average rainfall amount. The correlation coefficients are all low, i.e., 0.08 for the *KVS* value, -0.02 for the *KHT* value and 0.20 for the *KHS* value, respectively. However, it is observed that the *KVS* and *KHS* values slightly increase while the *KHT* value slightly decreases along with the increase of the average rainfall amount. With reference to the maximum rainfall intensity, a significant positive correlation (significance level $p < 0.01$) between the maximum rainfall intensity and the *KVS* value is found with the correlation coefficient of 0.76, while the correlations of the maximum rainfall intensity with the *KHT* and *KHS* values are relatively weak (significance level $p > 0.1$), with the correlation coefficients of 0.30 for the *KHT* value and 0.15 for the *KHS* value, respectively. However, all the three parameters increase along with the increase of the maximum rainfall intensity. Therefore, only the statistical equation to estimate the *KVS* value is established in this paper, based on the data of the 14 floods occurred during 2005-2007. In this paper, various functional forms, such as linear, logarithmic and exponential, have been attempted, and the relationship between the maximum rainfall intensity and the *KVS* value in this river basin can approximately be expressed as follows:

$$KVS = 6.59\ln(MRI) - 17.88 \qquad (3)$$

where *MRI* is the maximum rainfall intensity and *KVS* is the vertical saturated conductivity between the two soil layers. The R^2 value of Eq. (3) is 0.50.

Figure 6 shows the relationship between the maximum rainfall intensity and the *KVS* value. The solid black line shows the estimated *KVS* values by using Eq. (3), and the dash grey lines show the ranges of the *RE* values within $\pm 50\%$ because the R^2 value of Eq. (3) is equal to 0.50. The 4 floods occurred in 2008, which are used to validate the proposed equation, are also shown in Figure 6. It is observed that the range between the dash grey lines can basically cover the scatters including the four points representing the 4 floods occurred in 2008, which indicates Eq. (3) can well estimate the *KVS* value based on the maximum rainfall intensity. Table 5 lists the *KVS* values estimated by Eq. (3) as well as the corresponding *RE* values (in parentheses) for the 4 floods occurred in 2008 which are used for validation. However, there are four points lying outside the range between the dash grey lines in Figure 6. It is worth noting that the *KVS* values of three points are lower than 2.0 mm/hr, which indicates that the relatively lower *KVS* values may not be well estimated based on the maximum rainfall intensity.

Figure 7 shows the comparisons of the simulations using the calibrated and estimated *KVS* values against the observations for the 4 floods occurred in 2008. The *NSCE* values of the simulation results using the estimated *KVS* values are 0.65, 0.74, 0.24 and 0.83, respectively, which are all lower than those using the calibrated *KVS* values (i.e., 0.71, 0.92, 0.25 and 0.87). For the two floods in Figures 7(a) and 7(c), the simulation results using the calibrated and estimated *KVS* values are similar; and more significant differences between the simulation results using the calibrated and estimated *KVS* values can be observed in

Figures 7(b) and 7(d) due to the relatively larger *RE* values of the estimated *KVS* values for these two floods.

4.4. Discussion

In this paper, the case that the maximum rainfall intensity and the average rainfall amount are both considered as influencing factors is also analyzed, and the statistical equation to estimate the *KVS* value can be obtained by the multiple regression method.

$$KVS = 7.03\ln(MRI) - 0.75\ln(ARA) - 16.18 \quad (4)$$

where *ARA* is the average rainfall amount. The R^2 value of Eq. (4) is 0.58.

Figure 8 shows the comparisons of the *KVS* values estimated by Eq. (3) and Eq. (4) against the calibrated *KVS* values, and the scatters are evenly distributed beside the dash grey line. Although the R^2 value of Eq. (4) is higher than that of Eq. (3), the improvement in estimating the *KVS* value is limited. The *KVS* values estimated by Eq. (4) as well as the corresponding *RE* values (in parentheses) for the 4 floods in 2008 are also listed in Table 5. The improvements are more obvious for the *KVS* values overestimated by Eq. (3) (e.g., the *RE* values turn to 34% from 41% and 38% for the second and fourth floods, respectively). Moreover, it is worth noting that, for the flood occurred during August 4-15, 2006 (i.e., the circle point near the lower left corner), the *KVS* value estimated by Eq. (4) cannot be presented in this figure because it is a negative value (i.e., -0.4 mm/hr). To further investigate this problem, it is found that the *KVS* value estimated by Eq. (4) will be a negative value if the maximum rainfall intensity is lower than 16.6 mm/hr while the maximum rainfall intensity is 15.7 mm/hr for the flood occurred during August 4-15, 2006. In contrast, such threshold value of Eq. (3) is 15.1 mm/hr. This means that these two

equations will be invalid if the maximum rainfall intensity is lower than the corresponding threshold values.

Figure 9 shows the distribution of the *KVS* value associated with the rainfall patterns (i.e., the average rainfall amount and the maximum rainfall intensity in this paper), which is produced based on the data of the 14 floods occurred during 2005-2007. The *KVS* value generally shows the increasing trend with the increase of the maximum rainfall intensity but almost no trend with the increase of the average rainfall amount. For the 4 floods occurred in 2008, the *KVS* values can be identified from Figure 9 according to the average rainfall amount and the maximum rainfall intensity, which are also shown in Table 5. For the second and third floods, the improvements in estimating the *KVS* values are significant, i.e., the *RE* values turn to -19% and -5%, respectively. For the first flood, the *KVS* values estimated by Eq. (3), Eq. (4) and Figure 9 are more or less the same. Only for the fourth flood, the *KVS* value estimated by Figure 9 has a larger error than those estimated by Eq. (3) and Eq. (4). This indicates that mapping the distribution of hydrological parameters associated with the rainfall patterns can be regarded as another way to estimate the feasible hydrological parameters.

Furthermore, this paper has attempted to establish the relationships between the maximum rainfall intensity and the horizontal saturated conductivities (i.e., the *KHT* and *KHS* values) in this river basin. However, the R^2 values of the derived statistical equations (Eq. (5) and Eq. (6)) are quite low (i.e., 0.09 for the *KHT* value and 0.03 for the *KHS* value, respectively), which indicates that they may not be applicable to the future rainfall-runoff events. The estimated *KHT* and *KHS* values can be regarded as reference values only if there is no other option.

$$KHT = 2.42\ln(MRI) - 2.34 \quad (5)$$

$$KHS = 0.15\ln(MRI) - 0.11 \quad (6)$$

where *KHT* and *KHS* are the horizontal saturated conductivities of the two soil layers.

Nevertheless, this paper can provide a method to estimate the feasible hydrological parameters based on rainfall patterns (i.e., amount and intensity) in river basins with no long-term historical observations. However, the limitations of this paper should be fully aware, which are mainly related to the following four aspects. First, this method is area-dependent. For different river basins, the relationships between hydrological parameters and rainfall patterns should be reestablished based on the observed rainfall and streamflow data. Second, whether to select the average rainfall amount as an influencing factor when estimating the feasible hydrological parameters should be carefully considered because the improvement is limited, at least in this study area. Third, the method to estimate the *KVS* value in case of relatively lower rainfall intensity should be further investigated because the proposed statistical equations will be invalid in such case. Fourth, considering the weak relationships between the horizontal saturated conductivities and the rainfall patterns, the method to estimate these parameters should be further developed by other means.

5. Conclusions

This paper develops a hydrological parameter estimation method for river basins with no long-term historical observations based on the statistical relationships of hydrological parameters with rainfall patterns (i.e., amount and intensity). Regarding the Leli River basin as the study area, the findings of this paper can be described as follows:

First, the calibration parameters in the DYRIM are independently calibrated for each flood event using a double-layer parallel system, and the performances of the hydrological simulation results are evaluated by two ways, namely, separate evaluation for each flood event and comprehensive evaluation for a group of flood events. The results reveal that the simulation accuracy is generally high and can meet the national standards of China (MWR, 2000). Moreover, the value ranges of the calibration parameters are determined through identifying the maximum and minimum values.

Second, based on the correlation analysis between hydrological parameters and rainfall patterns (i.e., amount and intensity), the variables applicable for establishing the statistical relationships are determined and the statistical equations including the selected variables are developed. Moreover, the results reveal that mapping the distribution of hydrological parameters associated with the rainfall patterns can also provide a solution to the problem of estimating the necessary hydrological parameters with limited observations.

Overall, the proposed method is feasible in estimating hydrological parameters for future rainfall-runoff events in small and medium river basins such as the Leli River basin with no long-term historical observations. This will be valuable for making better decisions on flood control, integrated water resources management and ecological environment assessment in future.

Acknowledgements

This study was supported by the Natural Science Foundation of Qinghai Province project (Grant No. 2017-ZJ-911), the Natural Science Foundation of China project (Grant No. 51579131) and the Non-profit Fund Program of the Ministry of Water Resources of China (201501028). We are also grateful to the associate editor and the two anonymous reviewers who offered the insightful comments leading to improvement of this paper.

References

ASTER GDEM Validation Team, 2011. ASTER global DEM version 2 - summary of validation results. METI & NASA.

Athira, P., Sudheer, K.P., Cibin, R., Chaubey, I., 2016. Predictions in ungauged basins: an approach for regionalization of hydrological models considering the probability distribution of model parameters. *Stochastic Environmental Research and Risk Assessment*, 30(4), 1131-1149.

Bai, R., Li, T.J., Huang, Y.F., Li, J.Y., Wang, G.Q., 2015a. An efficient and comprehensive method for drainage network extraction from DEM with billions of pixels using a size-balanced binary search tree. *Geomorphology*, 238, 56-67.

Bai, R., Li, T.J., Huang, Y.F., Li, J.Y., Wang, G.Q., Yin, D.Q., 2015b. A hierarchical method for managing massive data of drainage networks extracted from high resolution DEM for large scale river basins. *Computers & Geosciences*, 85, 234-247.

Bardossy, A., 2007. Calibration of hydrological model parameters for ungauged catchments. *Hydrology and Earth System Sciences*, 11(2), 703-710.

Brassel, K.E., Reif, D., 1979. A procedure to generate Thiessen polygons. *Geographical Analysis*, 11, 289-303.

Bulygina, N., Ballard, C., McIntyre, N., O'Donnell, G., Wheater, H., 2012. Integrating different types of information into hydrological model parameter estimation: Application to ungauged catchments and land use scenario analysis. *Water Resources Research*, 48, W06519.

Chen, L., Xiang, L., Young, M.H., Yin, J., Yu, Z.B., van Genuchten, M.T., 2015. Optimal parameters for the Green-Ampt infiltration model under rainfall conditions. *Journal of Hydrology and Hydromechanics*, 63(2), 93-101.

Chinese Academy of Sciences, 1978. *Soil Map of China*. China Map Press, Beijing.

Choi, Y.S., Choi, C.K., Kim, H.S., Kim, K.T., Kim, S., 2015. Multi-site calibration using a grid-based event rainfall–runoff model: a case study of the upstream areas of the Nakdong River basin in Korea. *Hydrological Processes*, 29, 2089-2099.

Coff, B.E., Ditty, N.J., Gee, M.C., Szemis, J.M., Maier, H.R., Dandy, G.C., Gibbs, M.S., 2009. Relating catchment attributes to parameters of a salt and water balance model. *The 18th World IMACS Congress and MODSIM09 International Congress on Modelling and Simulation: Proceedings*, 3365-3371.

Fuentes-Andino, D., Beven, K., Kauffeldt, A., Xu, C.-Y., Halldin, S., Di Baldassarre, G., 2017. Event and model dependent rainfall adjustments to improve discharge predictions. *Hydrological Sciences Journal*, 62(2), 232-245.

Gao, Z., Long, D., Tang, G.Q., Zeng, C., Huang, J.S., Hong, Y., 2017. Assessing the potential of satellite-based precipitation estimates for flood frequency analysis in ungauged or poorly gauged tributaries of China's Yangtze River basin. *Journal of Hydrology*, doi: 10.1016/j.jhydrol.2017.05.025.

Garambois, P.A., Calmant, S., Roux, H., et al., 2017. Hydraulic visibility: Using satellite altimetry to parameterize a hydraulic model of an ungauged reach of a braided river. *Hydrological Processes*, 31(4), 756-767.

Garcia, M.G., Koike, T., 2016. Parameter-estimation methods for symmetric stable distributions: Application to small samples of spatial fluctuations of rainfall. *Spatial Statistics*, 17, 50-70.

Holland, J., 1975. *Adaptation in Natural and Artificial Systems*. University of Michigan Press, Ann Arbor, Michigan, USA.

Huang, P.N., Li, Z.J., Chen, J., Li, Q.L., Yao, C., 2016. Event-based hydrological modeling for detecting dominant hydrological process and suitable model strategy for semi-arid catchments. *Journal of Hydrology*, 542, 292-303.

Hundecha, Y., Ouarda, T.B.M.J., Bardossy, A., 2008. Regional estimation of parameters of a rainfall-runoff model at ungauged watersheds using the "spatial" structures of the parameters within a canonical physiographic-climatic space. *Water Resources Research*, 44(1), W01427.

Li, T.J., Wang, G.Q., Chen, J., 2010. A modified binary tree codification of drainage networks to support complex hydrological models. *Computers & Geosciences*, 36(11), 1427-1435.

Li, T.J., Wang, G.Q., Chen, J., Wang, H., 2011. Dynamic parallelization of hydrological model simulations. *Environmental Modelling & Software*, 26, 1736-1746.

Li, T.J., Wang, G.Q., Huang, Y.F., Fu, X.D., 2009. Modeling the process of hillslope soil erosion in the Loess Plateau. *Journal of Environmental Informatics*, 14(1), 1-10.

Li, X.H., Zhang, Q., Xu, C.Y., 2012. Suitability of the TRMM satellite rainfalls in driving a distributed hydrological model for water balance computations in Xinjiang catchment, Poyang lake basin. *Journal of Hydrology*, 426, 28-38.

Liu, Z.Y., Yang, D.W., Hu, J.W., 2010. Dynamic critical rainfall-based torrential flood early warning for medium-small rivers. *Journal of Beijing Normal University*, 46(3), 317-318. [In Chinese]

Maswood, M., Hossain, F., 2016. Advancing river modelling in ungauged basins using satellite remote sensing: the case of the Ganges-Brahmaputra-Meghna basin. *International Journal of River Basin Management*, 14(1), 103-117.

Merz, R., Blöschl, G., 2005. Flood frequency regionalisation—spatial proximity vs. catchment attributes. *Journal of Hydrology*, 302(1-4), 283-306.

Nash, J.E., Sutcliffe, J.V., 1970. River flow forecasting through conceptual models part 1 - A discussion of principles. *Journal of Hydrology*, 10(3), 282-290.

Pappenberger, F., Bartholmes, J., Thielen, J., Cloke, H.L., Buizza, R., Roo, A., 2008. New dimensions in early flood warning across the globe using grand-ensemble weather predictions. *Geophysical Research Letters*, 35(10), L10404.

Reshma, T., Reddy, K.V., Pratap, D., Ahmedi, M. Agilan, V., 2015. Optimization of calibration parameters for an event based watershed model using genetic algorithm. Water Resources Management, 29(13), 4589-4606.

Shi, H.Y., 2013. Computation of spatially distributed rainfall by merging raingauge measurements, satellite observations and topographic information: A case study of the 21 July 2012 rainstorm in Beijing, China. *The 35th IAHR World Congress*, Chengdu, China.

Shi, H.Y., Fu, X.D., Wang, H., Gong T.L., 2011. Modeling and prediction of water loss and soil erosion for high-relief mountainous region: case study of Qamdo region. *Journal of Basic Science and Engineering*, 19(S1), 17-27. (In Chinese)

Shi, H.Y., Li, T.J., Liu, R.H., Chen, J., Li, J.Y., Zhang, A., Wang, G.Q., 2015. A service-oriented architecture for ensemble flood forecast from numerical weather prediction. *Journal of Hydrology*, 527, 933-942.

Shi, H.Y., Li, T.J., Wang, K., Zhang, A., Wang, G.Q., Fu, X.D., 2016. Physically-based simulation of the streamflow decrease caused by sediment-trapping dams in the middle Yellow River. *Hydrological Processes*, 30(5), 783-794.

Shi, H.Y., Wang, G.Q., 2015. Impacts of climate change and hydraulic structures on runoff and sediment discharge in the middle Yellow River. *Hydrological Processes*, 29(14), 3236-3246.

Skaugen, T., Peerebom, I.O., Nilsson, A., 2015. Use of a parsimonious rainfall-run-off model for predicting hydrological response in ungauged basins. *Hydrological Processes*, 29(8), 1999-2013.

Soulis, K.X., Valiantzas, J.D., 2012. SCS-CN parameter determination using rainfall-runoff data in heterogeneous watersheds - the two-CN system approach. *Hydrology and Earth System Sciences*, 16(3), 1001-1015.

Sun, W.C., Ishidaira, H., Bastola, S., 2012. Calibration of hydrological models in ungauged basins based on satellite radar altimetry observations of river water level. *Hydrological Processes*, 26(23), 3524-3537.

Tang, L., Hossain, F., Huffman, G.J., 2010. Transfer of satellite rainfall uncertainty from gauged to ungauged regions at regional and seasonal time scales. *Journal of Hydrometeorology*, 11(6), 1263-1274.

The Ministry of Water Resources of China (MWR), 2000. Standard for hydrological information and hydrological forecasting SL250-2000. Beijing, China.

Thiessen, A.J., Alter, J.C., 1911. Precipitation Averages for Large Areas. *Monthly Weather Review*, 39, 1082-1984.

Tucker, C.J., Pinzon, J.E., Brown, M.E., Slayback, D.A., Pak, E.W., Mahoney, R., Vermote, E.F., El Saleous, N., 2005. An extended AVHRR 8-km NDVI dataset compatible with MODIS and SPOT vegetation NDVI data. *International Journal of Remote Sensing*, 26(20), 4485-4498.

Wagener, T., Wheater, H.S., 2006. Parameter estimation and regionalization for continuous rainfall-runoff models including uncertainty. *Journal of Hydrology*, 320(1-2), 132-154.

Wang, G.Q., Fu, X.D., Shi, H.Y., Li, T.J., 2015. Watershed sediment dynamics and modeling: a watershed modeling system for Yellow River. In Yang C.T. and Wang L.K. (eds), Advances in Water Resources Engineering, Handbook of Environmental Engineering, Volume 14, Chapter 1, 1-40. Springer Cham Heidelberg New York Dordrecht London.

Wang, G.Q., Wu, B.S., Li, T.J., 2007. Digital Yellow River model. *Journal of Hydro-environment Research*, 1(1), 1-11.

Wang, H., Fu, X.D., Wang, G.Q., Li, T.J., Gao, J., 2011. A common parallel computing framework for modeling hydrological processes of river basins. *Parallel Computing*, 37, 302-315.

Wang, H., Zhou, Y., Fu, X.D., Gao, J., Wang, G.Q., 2012. Maximum speedup ratio curve (MSC) in parallel computing of the binary-tree-based drainage network. *Computers &Geosciences*, 38, 127-135.

Woldemeskel, F.M., Sivakumar, B., Sharma, A., 2013. Merging gauge and satellite rainfall with specification of associated uncertainty across Australia. *Journal of Hydrology*, 499, 167-176.

Ye, J.Y., Wu, Y.T., Li, Z.J., Chang, L., 2012. Forecasting methods for flash floods in medium and small rivers in humid regions and their applications. *Journal of Hohai University (Natural Sciences)*, 40(6), 615-621. [In Chinese]

Yin, X.L., 2009. Study on scheduling of main reservoir on Pearl River for estuarine fresh water providing based on digital basin model. Ph.D. dissertation, Department of Hydraulic Engineering, Tsinghua University, Beijing, China. [In Chinese]

Yoo, C., Lee, J., Lee, M., 2017. Parameter estimation of the Muskingum Channel Flood-Routing Model in ungauged channel reaches. *Journal of Hydrologic Engineering*, 22(7), 05017005.

Yu, W., Nakakita, E., Kim, S., Yamaguchi, K., 2016. Improving the accuracy of flood forecasting with transpositions of ensemble NWP rainfall fields considering orographic effects. *Journal of Hydrology*, 539, 345-357.

Zhang, A., Li, T.J., Si, Y., Liu, R.H., Shi, H.Y., Li, X., Li, J.Y., Wu, X., 2016. Double-layer parallelization for hydrological model calibration on HPC systems. *Journal of Hydrology*, 535, 737-747.

Figures

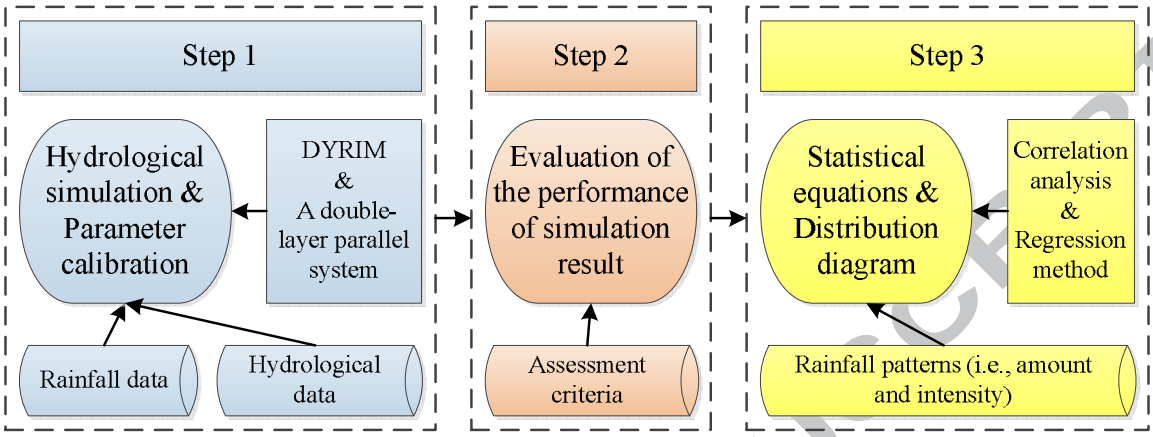

Figure 1. Flow chart of the hydrological parameter estimation method.

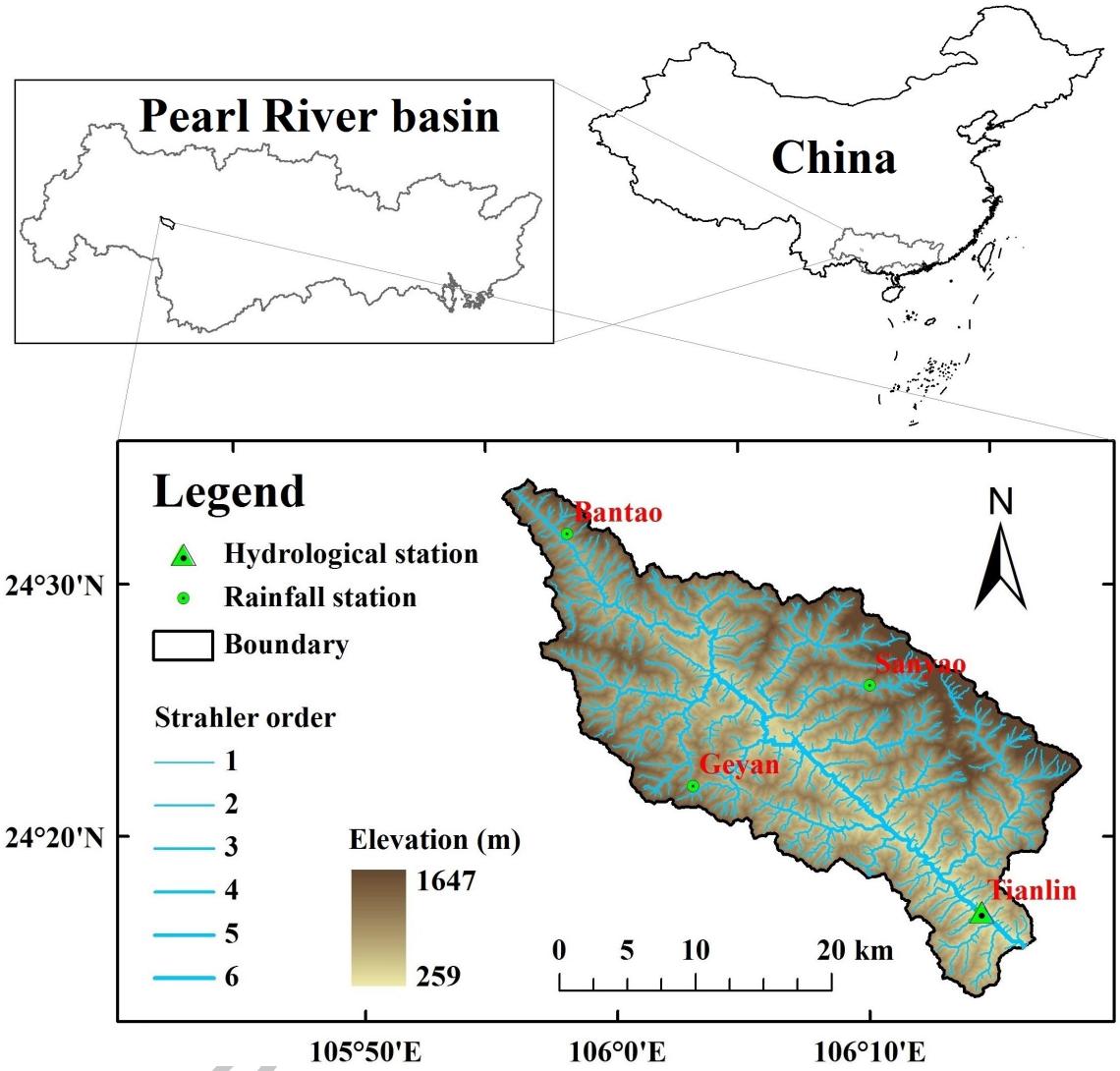

Figure 2. The locations of rainfall stations and hydrological station in the Leli River basin.

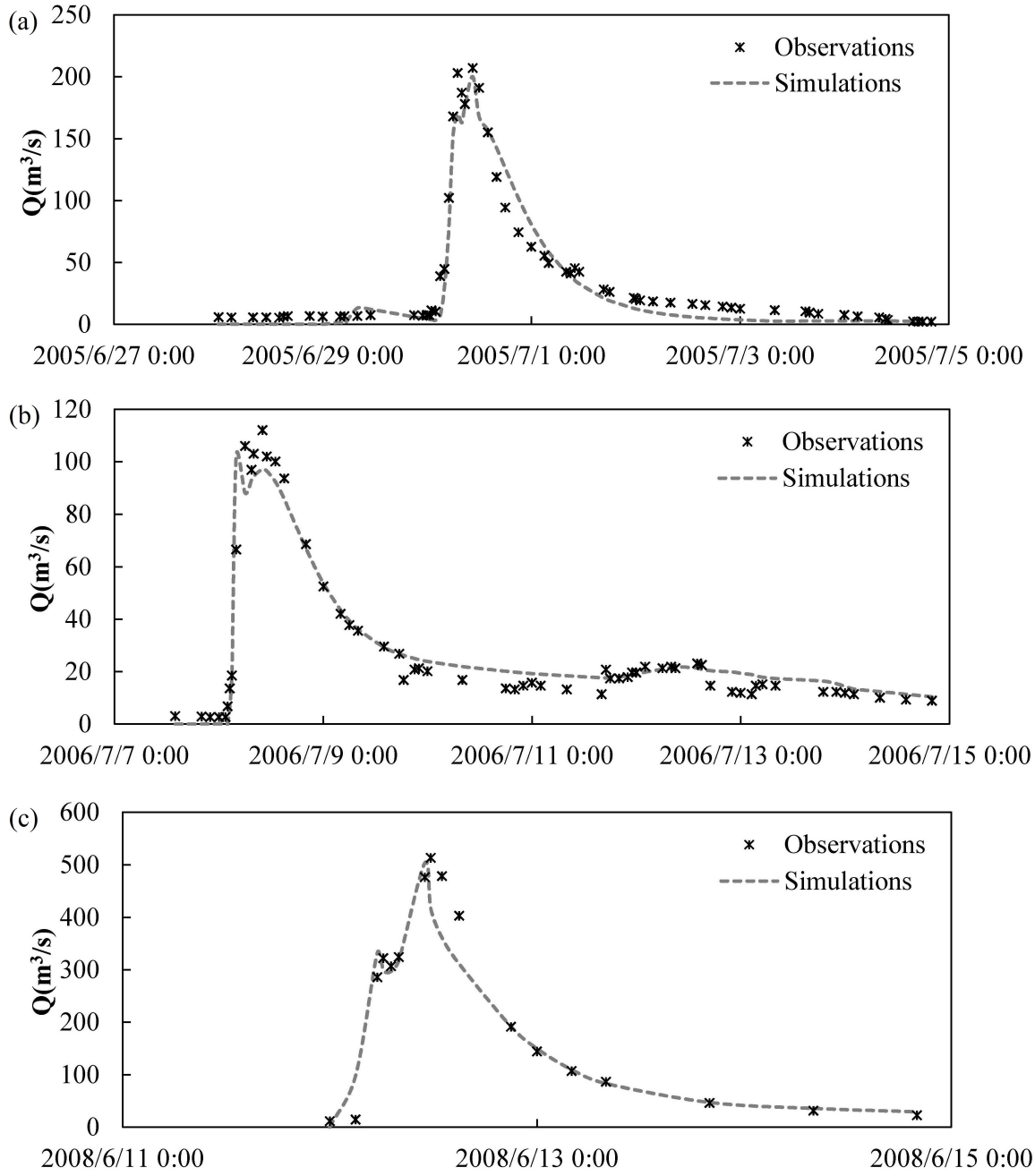

Figure 3. The comparisons of the simulations against the observations for the 3 floods with the *NSCE* values higher than 0.9.

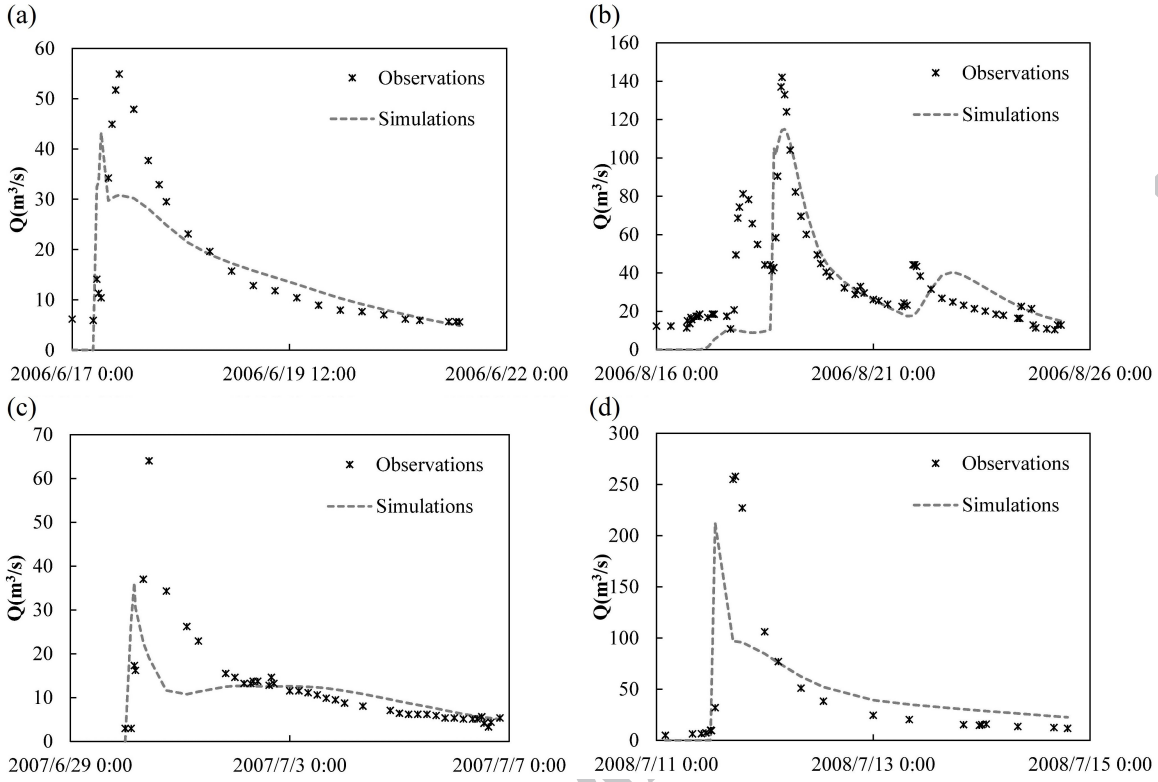

Figure 4. The comparisons of the simulations against the observations for the 4 floods with the *NSCE* values lower than 0.5.

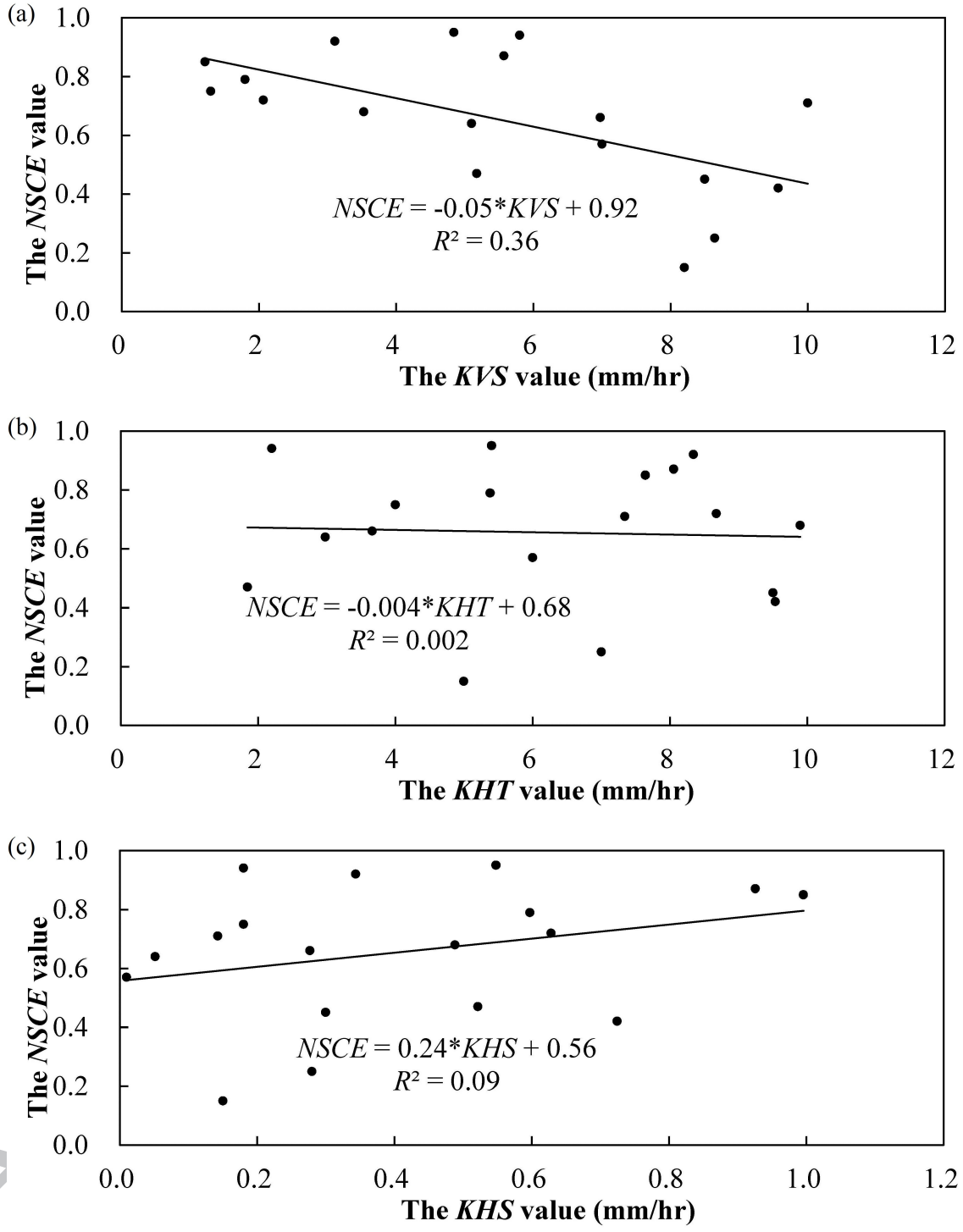

Figure 5. The relationships of the *NSCE* value with the *KVS*, *KHT* and *KHS* values.

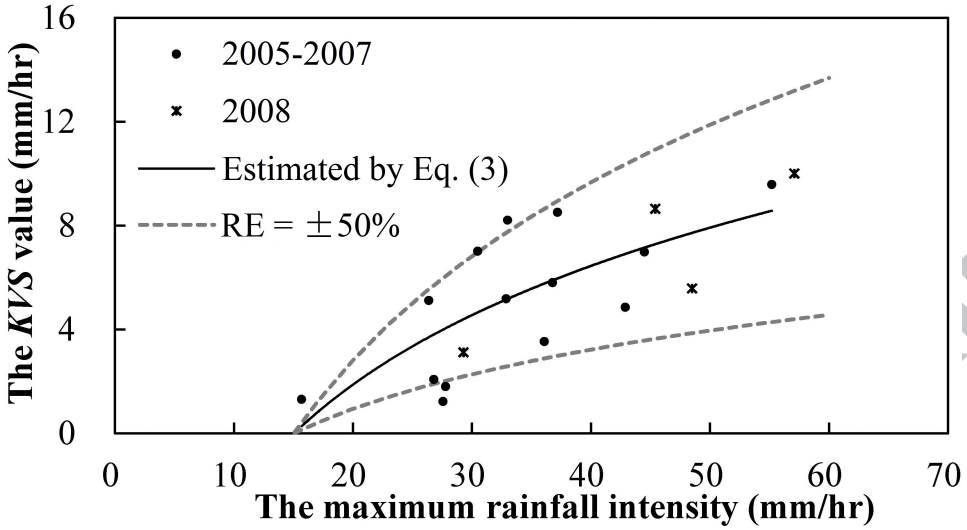

Figure 6. The relationship between the maximum rainfall intensity and the *KVS* value.

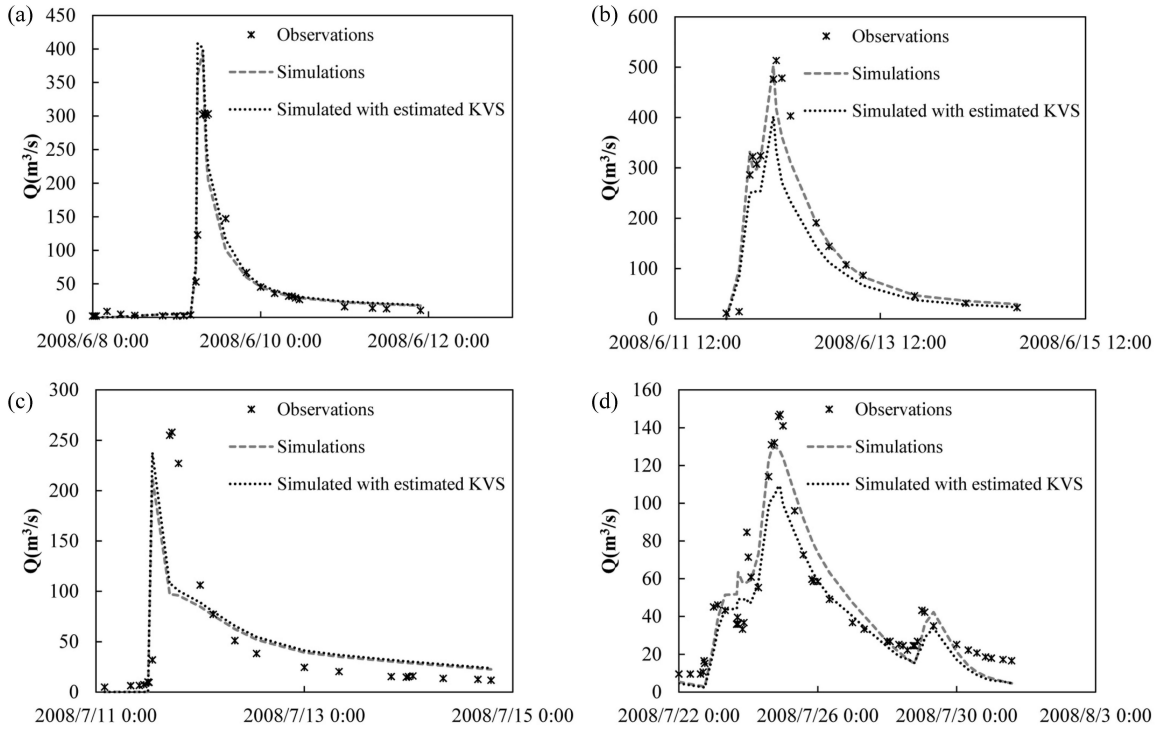

Figure 7. The comparisons of the simulations using the calibrated and estimated *KVS* values against the observations for the 4 floods occurred in 2008.

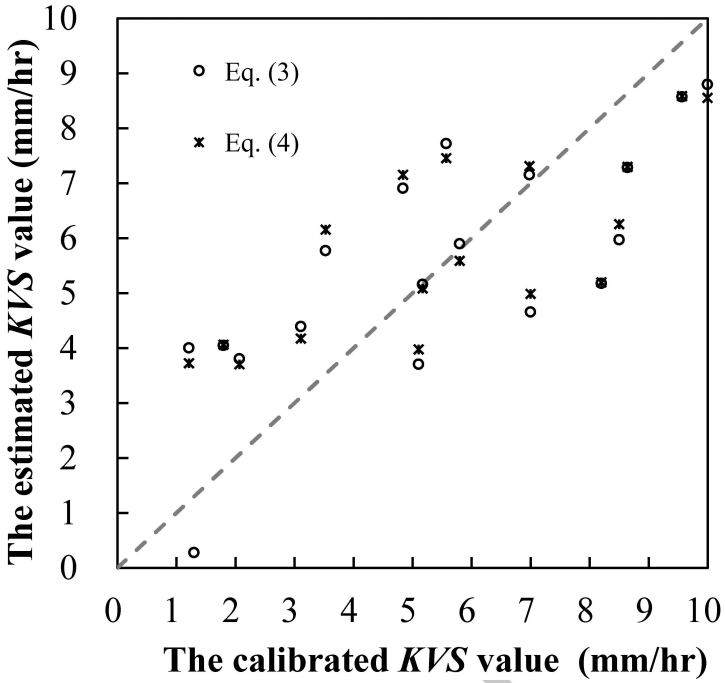

Figure 8. The comparisons of the *KVS* values estimated by Eq. (3) and Eq. (4) against the calibrated *KVS* values.

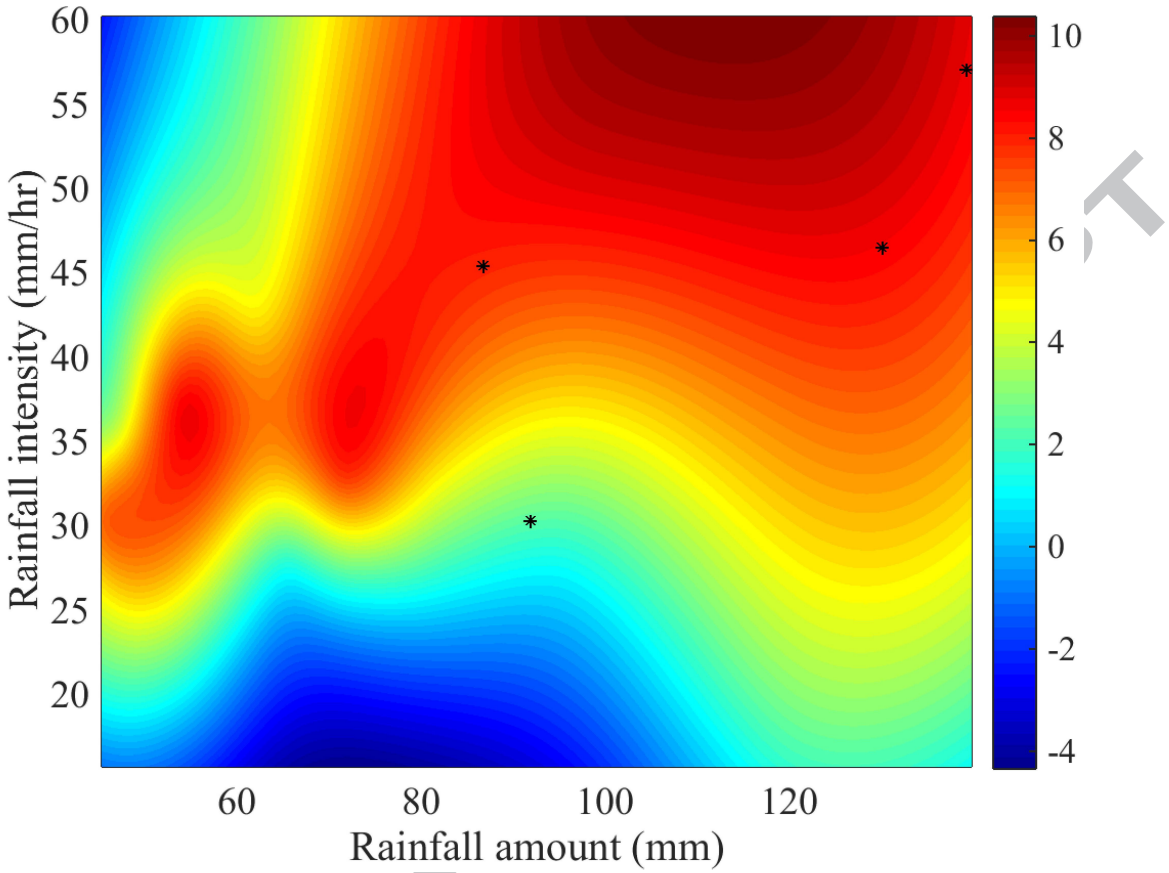

Figure 9. The distribution of the *KVS* value associated with the rainfall patterns. Note: the black points denote the 4 floods occurred in 2008.

Tables

Table 1. The physical parameters determined from the previous study on the Pearl River basin using the DYRIM (Yin, 2009)

Parameter	*CT1*	*CT2*	*CS1*	*CS2*	*D* (m)	*I* (m)
Value	0.212	0.296	0.1	0.13	0.5	0.0036

Table 2. The hydrological simulation results of all the 18 floods occurred during 2005-2008 in the Leli River basin

Year	Flood	*NSCE*	*REPF* (%)	*REFV* (%)
2005	6.20-6.27	0.72	-5	-24
	6.28-7.4	0.95	-3	-12
	8.21-8.26	0.66	11	-14
2006	6.13-6.16	0.64	-31	-23
	6.17-6.21	0.45	-21	-8
	7.7-7.14	0.94	-9	7
	7.15-7.24	0.51	-5	4
	8.4-8.15	0.75	1	-14
	8.16-8.25	0.42	-19	-12
2007	6.26-6.29	0.57	-1	53
	6.30-7.6	0.15	-44	-23
	7.11-7.19	0.79	-32	-3
	9.2-9.7	0.68	9	-6
	9.8-9.14	0.85	-19	-7
2008	6.8-6.11	0.71	31	-6
	6.12-6.14	0.92	-2	-6
	7.11-7.14	0.25	-17	12
	7.22-7.31	0.87	-11	-2
Mean value		0.66	-9	-5
Overall value		0.79	/	/

Table 3. The value ranges of the calibration parameters in the Leli River basin

Parameter	*KVS* (mm/hr)	*KHT* (mm/hr)	*KHS* (mm/hr)
Mean value	5.5	6.2	0.41
Maximum value	10.0	9.9	1.0
Minimum value	1.2	1.8	0.01
Standard deviation	2.8	2.5	0.3

Table 4. The average rainfall amount and the maximum rainfall intensity during the period of each flood in the Leli River basin

Year	Flood	Average rainfall amount (mm)	Maximum rainfall intensity (mm/hr)
2005	6.20-6.27	74.7	26.8
	6.28-7.4	62.0	42.9
	8.21-8.26	70.5	44.5
2006	6.13-6.16	45.3	26.4
	6.17-6.21	54.2	37.3
	7.7-7.14	118.4	36.8
	7.15-7.24	81.0	32.9
	8.4-8.15	120.0	15.7
	8.16-8.25	97.4	55.2
2007	6.26-6.29	45.6	30.5
	6.30-7.6	71.7	33.0
	7.11-7.19	65.5	27.8
	9.2-9.7	46.6	36.1
	9.8-9.14	95.7	27.6
2008	6.8-6.11	139.3	57.1
	6.12-6.14	91.9	29.3
	7.11-7.14	86.8	45.4
	7.22-7.31	130.3	48.5

Table 5. The *KVS* values estimated by Eq. (3), Eq. (4) and Figure 9 as well as the *RE* values (in parentheses) for the 4 floods occurred in 2008

Flood	*KVS* (mm/hr)			
	Calibrated	Estimated by Eq. (3)	Eq. (4)	Figure 9
6.8-6.11	10.0	8.8 (-12%)	8.6 (-14%)	8.77 (-12.3%)
6.12-6.14	3.1	4.4 (41%)	4.2 (34%)	2.51 (-19%)
7.11-7.14	8.6	7.3 (-16%)	7.3 (-16%)	8.19 (-5%)
7.22-7.31	5.6	7.7 (38%)	7.5 (34%)	8.48 (51%)

Research Highlights

1. Estimation of hydrological parameters with limited observed data
2. Comprehensive evaluation of simulation results as a group of events
3. Establishment of statistical equations based on rainfall patterns
4. Mapping the distribution of hydrological parameters with rainfall patterns